

## Molecular Crystals and Liquid Crystals Science and Technology. Section A. Molecular Crystals and Liquid Crystals

Publication details, including instructions for authors and  
subscription information:

<http://www.tandfonline.com/loi/gmcl19>

### Dopant Effects on Electro-Thermo- Optical Characteristics in Matrix- addressed Smectic-A Liquid Crystal Displays

Hitoshi Hatoh<sup>a</sup>

<sup>a</sup> Electron Device Engineering Laboratory, Toshiba Corporation,  
8, Shinsugita-cho, Isogo-ku, Yokohama, 235, Japan

Version of record first published: 24 Sep 2006.

To cite this article: Hitoshi Hatoh (1994): Dopant Effects on Electro-Thermo-Optical  
Characteristics in Matrix-addressed Smectic-A Liquid Crystal Displays, Molecular Crystals and  
Liquid Crystals Science and Technology. Section A. Molecular Crystals and Liquid Crystals, 250:1,  
1-13

To link to this article: <http://dx.doi.org/10.1080/10587259408028187>

PLEASE SCROLL DOWN FOR ARTICLE

Full terms and conditions of use: <http://www.tandfonline.com/page/terms-and-conditions>

This article may be used for research, teaching, and private study purposes. Any  
substantial or systematic reproduction, redistribution, reselling, loan, sub-licensing,  
systematic supply, or distribution in any form to anyone is expressly forbidden.

The publisher does not give any warranty express or implied or make any  
representation that the contents will be complete or accurate or up to date. The  
accuracy of any instructions, formulae, and drug doses should be independently  
verified with primary sources. The publisher shall not be liable for any loss, actions,  
claims, proceedings, demand, or costs or damages whatsoever or howsoever caused  
arising directly or indirectly in connection with or arising out of the use of this material.

# Dopant Effects on Electro-Thermo-Optical Characteristics in Matrix-addressed Smectic-A Liquid Crystal Displays

HITOSHI HATOH

*Electron Device Engineering Laboratory, Toshiba Corporation, 8, Shinsugita-cho, Isogo-ku, Yokohama, 235 Japan*

*(Received December 9, 1992; in final form February 26, 1993)*

Liquid crystal (LC) materials doped with non-mesomorphic or chiral substances are used for the matrix-addressed LC displays based on electro-thermo-optical effect. The influence of phase-transition temperature on driving condition and contrast ratio is investigated.

Non-mesomorphic dopants which decrease greatly the thermal stability of LC phase expands the allowance of the driving condition and increases the contrast ratio. The chiral dopants also cause similar effects. However, the effects are not caused by the decrease of the thermal stability but by the twist force of chiral dopants.

The minimum signal voltage to make a transparent state is not changed by non-mesomorphic dopant, whereas it increases with increasing the concentration of the chiral dopant.

On the basis of our investigation, LC blends with the non-mesomorphic or chiral dopants have been developed. They have not only a wide allowance of driving condition and a high contrast ratio but also a high writing speed.

*Keywords: electro-thermo-optical effect, smectic-A, matrix addressing, dopant*

## 1. INTRODUCTION

Electro-thermo-optical effect matrix-addressed liquid crystal displays (LCDs)<sup>1</sup> have a capability to display a large information content. These displays show no cross-talk effect even under a highly multiplexing drive, since two different activating forces, i.e., thermal energy and signal voltage, are used for the row and column electrodes during driving.

In order to improve the display performance of an LCD, it is important to improve the LC material as well as to optimize cell configuration and driving conditions. In the case of laser-addressed LCDs,<sup>2,3</sup> it is known that doping the LC material with some dopants improves the contrast ratio. In this paper, the influence of the phase transition temperature change on the driving condition and the contrast ratio is investigated when LC materials doped with non-mesomorphic or chiral substances are used for the electro-thermo-optical effect matrix-addressed LCD.

## 2. OPERATION PRINCIPLE

A liquid crystal material used in an electro-thermo-optical effect LCD shows a smectic-A ( $S_A$ ) phase at room temperature. At a higher temperature, it changes to the nematic (N) phase. The temperature range for the nematic phase is relatively narrow, and further increasing the temperature, changes it to the isotropic (I) phase. Two substrates of a cell have heater electrodes and signal electrodes with a homeotropic alignment layer, respectively.

The LCD is operated by a combination of a heat pulse and a signal pulse as shown in Figure 1. A heat pulse is applied to the heater electrode so that the temperature of a liquid crystal is increased to the isotropic phase. The temperature begins to decrease after the removal of the heat pulse. When no signal voltage is applied to the cell during the nematic phase in the cooling process, a random molecular orientation of the isotropic phase is frozen in the  $S_A$  phase. Consequently, a forcal-conic orientation is generated and a scattering state is obtained. When a signal voltage is applied during the nematic phase as shown in Figure 1, LC molecules orient perpendicular to the substrates and a transparent state is obtained. Thus, by properly choosing the driving conditions, a scattering or transparent state can be obtained. The scattering or transparent state so obtained is not altered by application of the signal voltage as long as the LC material is in the  $S_A$  phase.

Display performance of the LCD is greatly influenced by the phase-transition temperature of the LC material. In the case of an LC material with a relatively high phase-transition temperature, a high thermal energy is required to heat the LC material to its isotropic phase. This means that the LCD needs a high heating power. If the heating power is restricted, the writing speed of the LCD is reduced. However, an LC material with a high phase-transition temperature has an advantage of high contrast ratio, because the temperature decrease from the isotropic phase is rapid and the random molecular orientation is effectively frozen. In the case of an LC material with a low phase-transition temperature, the required heating power is relatively low and the writing speed may be high, but its contrast ratio is low and the allowance of the driving condition is narrow.

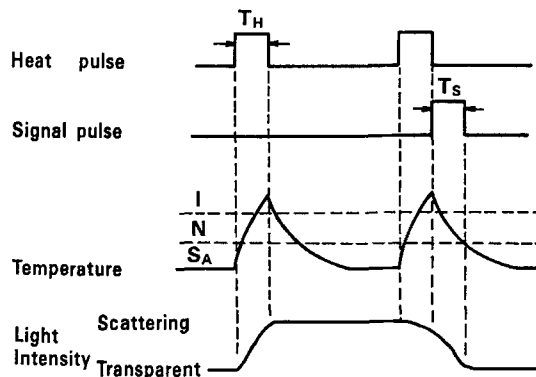




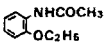
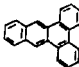
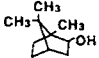
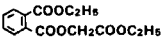
FIGURE 1 Waveforms of heat pulse and signal pulse applied to an electro-thermo-optical effect matrix-addressed LCD and its operation principle.

The aim of this study is to increase the contrast ratio and the allowance of the driving condition of an LCD without compromising its writing speed or without increasing the heating power. To achieve this goal, we have examined the effect of doping an LC material having a low phase-transition temperature with various non-mesomorphic and chiral dopants.

### 3. EXPERIMENTAL

An LC material termed CB-1, which is a mixture of 4-cyano-4'-*n*-decylbiphenyl (10 CB) and 4-cyano-4'-*n*-octylbiphenyl (8 CB) with molar proportions of 42:58, was used as the host material. It has a relatively low phase-transition temperature,  $S_A -42.1^\circ\text{C} - N - 46.6^\circ\text{C} - I$ . The CB-1 was doped with various dopants shown in Table I at various mole fractions  $x$ . The dopants from AAMS to *n*-D in Table I

TABLE I  
Examined dopants and their evaluated results

DOPANT	m.p. ( $^\circ\text{C}$ )	$\beta^N$	$\beta^I$	$\Delta\beta$	$\Delta t_H^*$	CR <sup>*</sup>
<b>AAME</b> Acetylsalicylic Acid Methyl Ester 	50	0.598	0.472	0.126	1.8	50
<b>Adm</b> Adamantane 	270	0.393	0.314	0.079	0.8	38
<b>APT</b> o-Acetylphenetidine 	79	0.566	0.456	0.110	1.4	45
<b>Bnz</b> 2,3-Benztriphenylene 	206	0.126	0.115	0.011	0.2	23
<b>Brn</b> Borneol 	204	0.425	0.330	0.095	1.4	44
<b>EPEG</b> Ethyl Phthalyl Ethyl Glycolate 	20	0.829	0.514	0.315	2.3	55
<b>n-D</b> n-Decane $\text{CH}_3(\text{CH}_2)_8\text{CH}_3$	-30	0.210	0.189	0.021	0.6	31
<b>CM-20</b> $\text{C}_2\text{H}_5-\overset{*}{\underset{\text{CH}_3}{\text{CH}}}-\text{CH}_2-\text{C}_6\text{H}_4-\text{C}_6\text{H}_4-\text{CO}-\text{C}_6\text{H}_4-\text{C}_9\text{H}_{11}$	128	-0.231	-0.262	0.031	1.5	46
<b>CB-15</b> $\text{C}_2\text{H}_5-\overset{*}{\underset{\text{CH}_3}{\text{CH}}}-\text{CH}_2-\text{O}-\text{C}_6\text{H}_4-\text{C}_6\text{H}_4-\text{CN}$	4	0.115	0.115	0	1.8	35

※ :  $P_H=40\text{W}$ ,  $x=0.02$

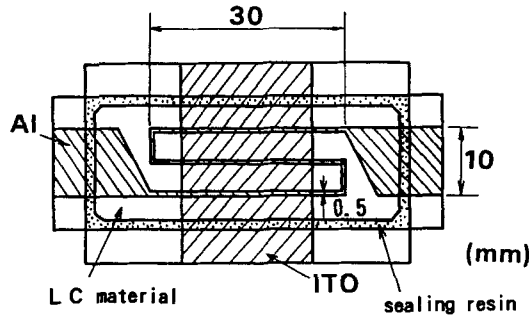


FIGURE 2 An LC cell used in a measurement of electro-thermo-optical characteristics.

are non-mesomorphic materials. The dopants CM-20 (obtained from Chisso Corp.) and CB-15 (obtained from E. Merck) are chiral liquid crystals. The phase-transition temperatures of mixtures were measured using a polarizing microscope to observe the phase transition during heating. The heating rate during these measurements was maintained at  $1.0^{\circ}\text{C}/\text{min}$  using a Mettler's thermal analysis system.

Figure 2 shows a schematic drawing of the plane view of the cell used in the measurements of the electro-thermo-optical characteristics. An aluminum heater electrode and an ITO signal electrode were patterned on separate substrates as shown in the figure. The thickness of the aluminum electrode was about 150 nm. A mono-carboxylatochromium complex<sup>4</sup> was used as a homeotropic alignment layer. The cell thickness was controlled from 7.8 to 8.2  $\mu\text{m}$  by mixing a glass fiber spacer in sealing resin. The electric resistance of the heater electrode was about 50  $\Omega$ .

The heat and signal pulses shown in Figure 1 were applied to the cells. At first, a heat pulse width  $t_H$  (ms), which can make a scattering state, was measured for each heat power  $P_H(W)$  without applying the signal pulse. Secondly, the contrast ratio CR was measured for each heat power  $P_H$ . The contrast ratio CR was defined as the ratio of luminances in the scattering state to that in the transparent state when the LC panel was illuminated by a halogen lamp light at an angle of  $45^{\circ}$  to the normal to the LC panel.

Once the scattering state was obtained using the heat pulse, a signal pulse of height  $V_S(V)$  was applied to obtain a transparent state. The minimum signal pulse width  $t_{S1}$  (ms) to obtain a transparent state for various voltage  $V_S$  was measured keeping  $P_H$  and  $t_H$  constant. Similarly minimum voltage  $V_{S1}$  to obtain a transparent state was measured by a given width  $t_S$  (ms) keeping  $P_H$  and  $t_H$  constant.

## 4. RESULTS AND DISCUSSION

### 4.1. Phase-transition Temperature

Figure 3(a) shows a phase diagram for the Brn - CB-1 system. The increasing Brn concentration decreases the smectic-nematic phase-transition temperature  $T_{SN}$ , as well as the nematic-isotropic phase-transition temperature  $T_{NI}$ . In addition, the

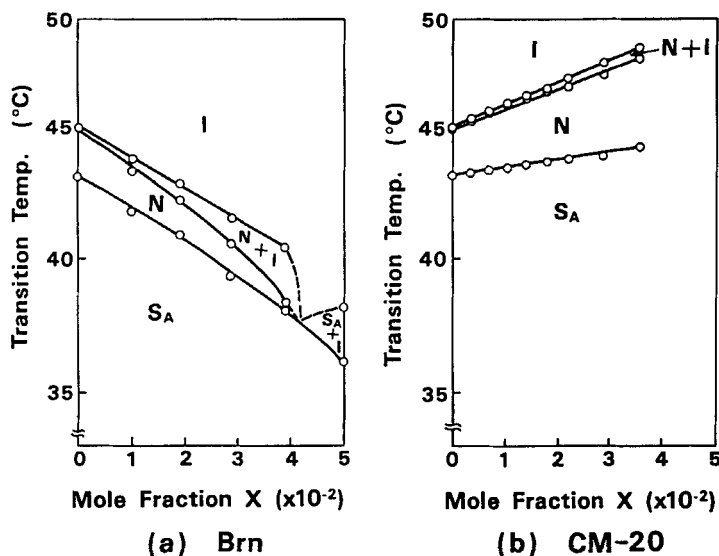


FIGURE 3 Phase diagrams of CB-1 doped with Brn (a) and CM-20 (b).

doping expands the temperature range in which the nematic and the isotropic phases coexist. This means that the Brn doping to CB-1 decreases the thermal stability of LC phase, and leads to a reduction of the nematic order. Doping of CB-1 with other non-mesomorphic materials shown in Table I also showed a similar effect to the Brn doping, though the degree of the effect depends on the kind of dopant materials. In the case of the CB-1 doped with chiral materials, such as CM-20 and CB-15, there was no effect on the thermal stability of LC phase. For example, Figure 3(b) shows a phase diagram for the CB-1 doped with CM-20. Considering that the clearing point of CM-20 is 128°C, the CB-1 doped with CM-20 seems to be an ordinary mixing between liquid crystals.

In order to evaluate the doping effect on the thermal stability of LC phase, we introduce the parameters  $\beta^N$ ,  $\beta^I$  and  $\Delta\beta$  which are defined as follows.<sup>5</sup>

$$\beta^N = [(1 - T(x)/T(x = 0))/x]^N \quad (1)$$

$$\beta^I = [(1 - T(x)/T(x = 0))/x]^I \quad (2)$$

$$\Delta\beta = \beta^N - \beta^I. \quad (3)$$

where  $x$  is the mole fraction of a dopant and  $T(x)$  is the phase-transition temperature corresponding to mole fraction of a dopant  $x$ . The superscription <sup>N</sup> denotes the transition from the nematic phase to a coexisting nematic-isotropic phase, and the superscription <sup>I</sup> denotes the transition from a coexisting nematic-isotropic phase to an isotropic phase. Based on the above formula, the higher the value of  $\beta$ , the lower the stability of LC phase. The parameter  $\Delta\beta$  quantifies the expansion of the temperature range of the coexisting nematic-isotropic phase and reduction of the nematic order.

Calculated values of the parameters  $\beta^N$ ,  $\beta^I$  and  $\Delta\beta$  for each dopant at  $x = 0.02$  are listed in Table I. The dopants EPEG, AAMS and APT show large  $\beta^N$ ,  $\beta^I$  and  $\Delta\beta$  values. Thus, they have a large effect on the reduction of the nematic order of LC material. The other dopants, *n*-D and Bnz, were found to have small values of  $\beta^N$ ,  $\beta^I$  and  $\Delta\beta$ . It is believed that the difference in the molecular shapes of a liquid crystal material and a dopant causes the reduction in the thermal stability of LC phase.

#### 4.2. Heat Power and Heat Pulse Width

Figures 4(a)–(d) are microphotographs showing a creation of scattering states when heat pulse width  $t_H$  is changed, while keeping  $P_H = 40$  W. The LC material was the CB-1 doped with Brn at  $x = 0.02$ . Figure 4(a) shows an initial transparent

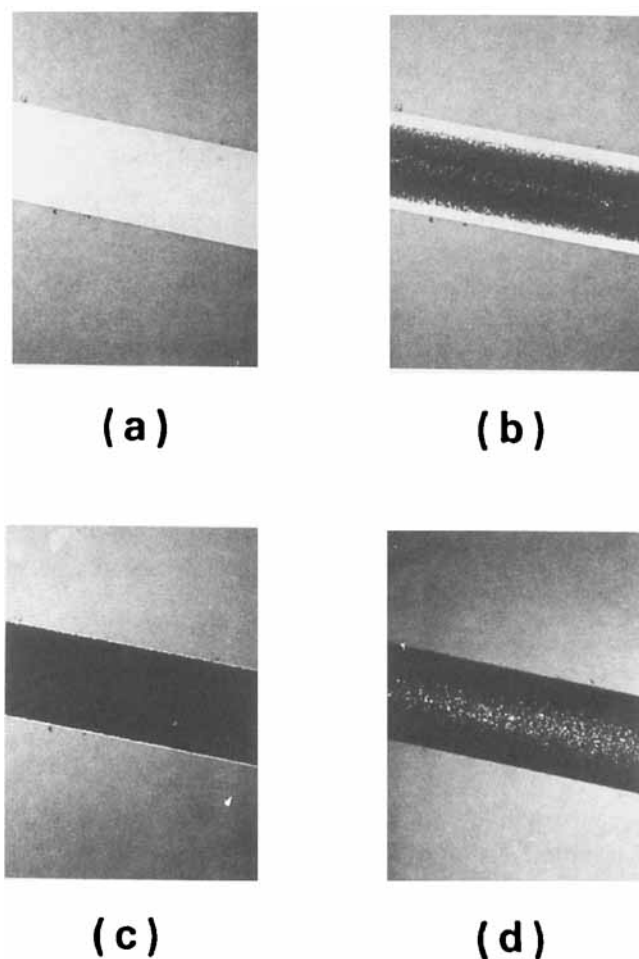


FIGURE 4 Creation of scattering states when heat pulse width  $t_H$  is changed (heat power  $P_H = 40$  W, Brn doping at  $x = 0.02$ ): (a) an initial transparent state; (b)  $t_H = 8.5$  ms; (c)  $t_H = 17$  ms; (d)  $t_H = 27$  ms.

state before an application of a heat pulse. The bright stripe in the figure is the heater electrode. Figure 4(b) shows the scattering or transparent state caused by a heat pulse width  $t_H$  of 8.5 ms. The dark region in the middle of the heater electrode is a scattering state with a focal-conic LC orientation. A transparent state remains in a bright area near the edge of the dark region. In this case, the LC material only in the middle of the heater electrode is heated to the isotropic phase because the heat pulse width is smaller than its optimum value. Figure 4(c) corresponds to a heat pulse width of 17 ms. The whole heater region shows the scattering state. In this case, the heat pulse width is an adequate value. In Figure 4(d), which corresponds to a heat pulse of 27 ms, a bright region is observed in the middle of the heater electrode. In this case, the heat pulse width is so long that the temperature decreased slowly and the LC molecules aligned homeotropically in the nematic phase by the effect of the alignment layer of the substrate.

Thus there is an optimum range of heat pulse width ( $t_{H1} - t_{H2}$ ) to achieve a scattering state in the whole heater electrode region for a given heat power  $P_H$ .

The relationship between the heat power and the heat pulse width is shown in Figure 5 for Brn doping at  $x = 0.02$ . The open circles correspond to  $t_{H1}$  and the closed circles correspond to  $t_{H2}$ . Although it is natural to consider that  $t_{H1}$  is inversely proportional to  $P_H$ , the measured  $t_{H1}$  was larger than the expected value. This may be due to heat loss by thermal conduction and diffusion in the cell.

The optimum heat pulse width for a given heat power changes with the concentration of dopants. Figures 6(a), (b), (c) and (d) show the Brn dopant concentration dependence of the heat pulse width for the heat powers of 30, 40, 50 and 60 W, respectively. The shaded region in the figures correspond to the range of the optimum heat pulse width. In the case of undoped CB-1 ( $x = 0$ ), the optimum heat pulse width has almost no allowance for all heat powers, as can be seen in the figures. The Brn doping to CB-1 expands the allowance of the driving condition. This is an advantage when a temperature distribution exists in the cell.

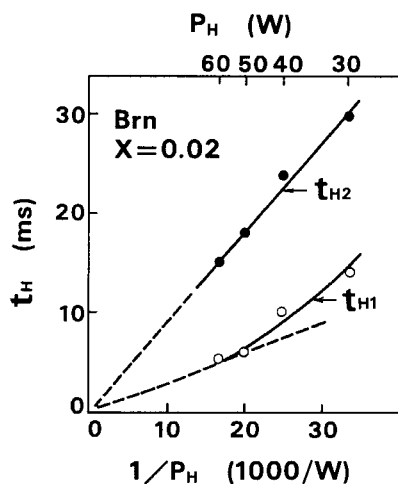


FIGURE 5 Heat power  $P_H$  vs. heat pulse width  $t_H$ .



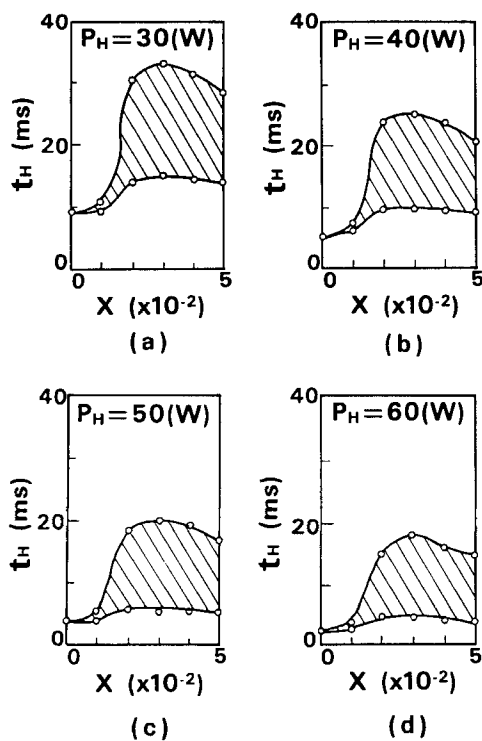


FIGURE 6 A doping concentration dependence of the optimum range of the heat pulse width (CB-1 doped with Brn).

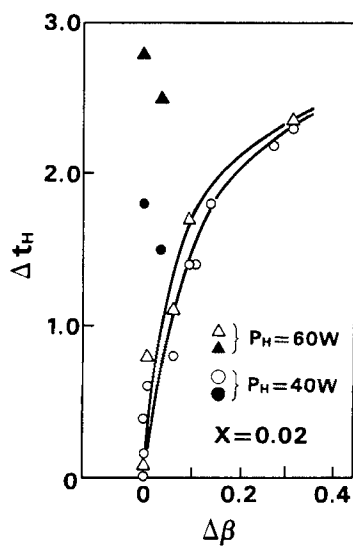


FIGURE 7  $\Delta\beta$  vs.  $\Delta t_H$ . Triangles correspond to chiral dopants and circles correspond to non-mesomorphic dopants.

In order to quantify the allowance of the driving condition, we introduce a heating margin parameter  $\Delta t_H$ , defined as follows:

$$\Delta t_H = t_{H2}/t_{H1} - 1. \quad (4)$$

The calculated values of  $\Delta t_H$  at  $x = 0.02$  is plotted against  $\Delta\beta$  values for various dopants as shown in Figure 7. The heat powers were 40 and 60 W. The open circles correspond to non-mesomorphic dopants and the closed circles correspond to chiral dopants. In the case of non-mesomorphic dopants,  $\Delta t_H$  increases with increasing  $\Delta\beta$ . We believe that the reduction of the nematic order on doping with non-mesomorphic dopants greatly contributes to the creation of the scattering state. In the case of chiral dopants, the relationship between  $\Delta t_H$  and  $\Delta\beta$  is not similar to that for non-mesomorphic dopants. In this case, the twist force of chiral dopants mainly contributes to the creation of the scattering state.

#### 4.3. Contrast Ratio CR

The dependence of the contrast ratio (CR) on heat power is shown in Figure 8 for CB-1 doped with Brn. The applied heat pulse width was an average value of  $t_{H1}$  and  $t_{H2}$  for each heat power. The contrast ratio increases with an increase in heat power. The similar results are obtained for other dopants as well.

Figures 9(a), (b), (c) and (d) show a doping concentration dependence of the contrast ratio for heat power of 30, 40, 50, and 60 W, respectively. The solid lines correspond to Brn doping and the broken lines correspond to Bnz doping. In the case of Brn doping, the contrast ratio increases with increasing the dopant concentration for every  $P_H$ . On the other hand, the Bnz doping does not have much effect on the contrast ratio.

The increase in the contrast ratio upon increasing the doping concentration depends on the kind of dopant, i.e. a non-mesomorphic dopant or a chiral dopant. It was found that the contrast ratio is related to the  $\Delta\beta$  value. Figure 10 plots  $\Delta\beta$

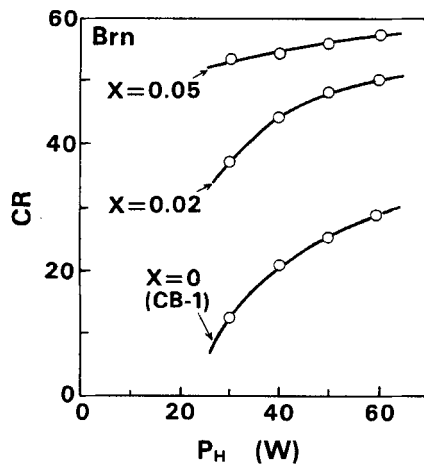


FIGURE 8 Heat power  $P_H$  vs. contrast ratio CR.

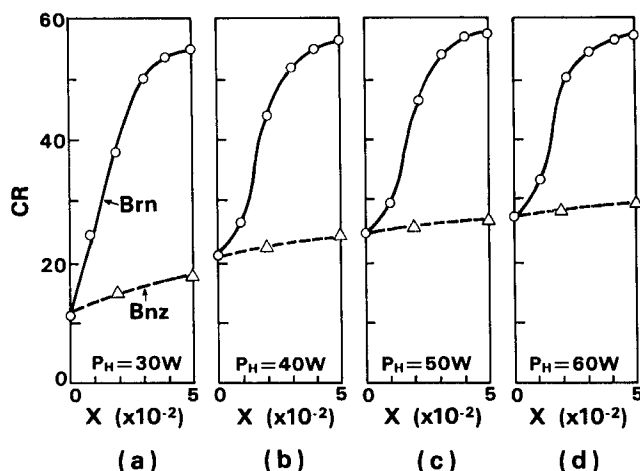


FIGURE 9 A dopant concentration dependence of contrast ratio CR for CB-1 doped with Brn and Bnz.

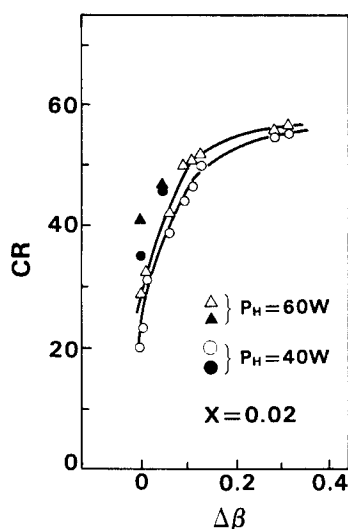


FIGURE 10  $\Delta\beta$  vs. CR. Triangles correspond to chiral dopants and circles correspond to non-mesomorphic dopants.

versus CR for each kind of dopant at  $x = 0.02$ . Closed symbols correspond to the non-mesomorphic dopants and open symbols correspond to the chiral dopants. In the case of the non-mesomorphic dopants, the contrast ratio increases with increasing  $\Delta\beta$ . It is easily recognized that a dopant which shows a low solubility in the nematic phase has a large effect on increasing the contrast ratio and on increasing the heating margin parameter,  $\Delta t_H$ .

The correlation between  $\Delta\beta$  and CR for the chiral dopants does not agree with that for the non-mesomorphic dopants. This suggests that there is a difference in the creation mechanism of the scattering state between non-mesomorphic dopants

and chiral dopants as was stated earlier. In the former case, the reduction of nematic order brings the scattering state, while, in the latter case, the twist force of chiral dopants brings the scattering state.

#### 4.4. Signal Pulse Width and Height

Figure 11 shows a plot of signal pulse height,  $V_s$ , versus the minimum signal pulse width,  $t_{s1}$ , for Brn doping at  $x = 0.02$  and  $P_H = 40$  W and 60 W. The minimum heat pulse width,  $t_{H1}$ , corresponding to each heat power was chosen in this plot. There is no change in  $t_{s1}$  even when the heat power or signal pulse height is changed. Similar results were obtained for other doping concentrations as well as other dopants. The minimum signal pulse width  $t_{s1}$  is thought to be a time for the temperature of liquid crystals to pass the nematic range. The nematic range passing time is thought to be almost independent of  $P_H$ , as long as the minimum heat pulse width  $t_{H1}$  is used for each heat power  $P_H$ . So it is natural that  $t_{H1}$  is independent of  $P_H$  and  $V_s$ .

On the other hand, the minimum signal voltage  $V_{s1}$  to make a transparent state depends on the kind of dopant as well as the doping concentration. Figure 12 shows doping concentration dependence of  $V_{s1}$  for Brn, CM-20 and CB-15 dopants. In the case of non-mesomorphic Brn,  $V_{s1}$  is independent of the doping concentration. Similar results were obtained in the case of other non-mesomorphic dopants. On the other hand, in the cases of chiral dopants CM-20 and CB-15,  $V_{s1}$  increases with increasing the dopant concentration. The difference in the doping concentration dependence of  $V_{s1}$  between these two cases also implies that there is a difference in the mechanism of electro-thermo-optical effects between the non-mesomorphic dopants and the chiral dopants.

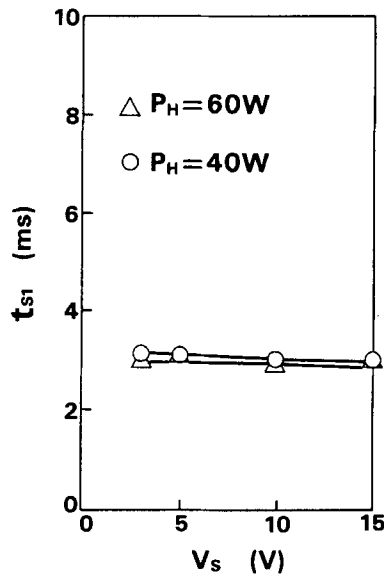


FIGURE 11 Signal pulse height  $V_s$  vs. the minimum signal pulse width  $t_{s1}$  (CB-1 doped with Brn at  $x = 0.02$ ).

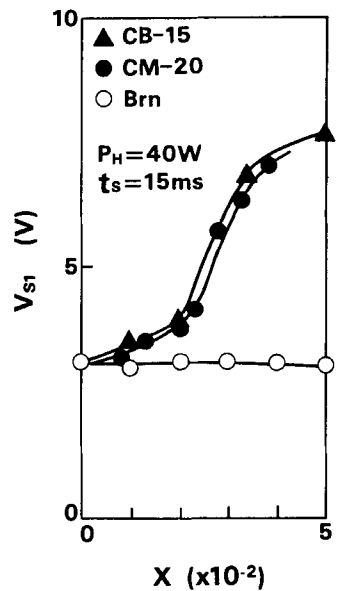


FIGURE 12 A doping concentration dependence of the minimum signal pulse width  $V_{S1}$  (CB-1 doped with CM-20, CB-15 and Brn,  $P_H = 40\text{ W}$ ,  $t_s = 15\text{ ms}$ ).

TABLE II  
Electro-thermo-optical characteristics of developed liquid crystal blends

	Mole fraction $X$	$T_{SN}$ ( $^{\circ}C$ )	$T_{N-NI}$ ( $^{\circ}C$ )	$T_{NI-I}$ ( $^{\circ}C$ )	$t_{H1}$ (ms) $P_H=40W$	$\Delta t_H$ $P_H=40W$	CR $P_H=40W$	$t_{S1}$ (ms)	$V_{S1}$ (V)
CB-1	—	43.1	44.8	44.9	6	0	22	3	3
CB-11 CB-1+EEEG	0.01	39.7	42.1	44.1	6	2.0	54	3	3
CB-12 CB-1+CM-20	0.02	43.8	46.3	46.6	10	1.5	46	3	4
CB-2	—	54.2	57.6	59.8	28	0.3	44	3	3

5. PERFORMANCE OF DEVELOPED LC BLENDS

On the basis of these investigations, liquid crystal blends CB-11 and CB-12 were developed. Their characteristics are listed in Table II. The former contains EPEG which has the largest  $\Delta\beta$  value among the non-mesomorphic dopants. The latter consists of CB-1 and the chiral dopant CM-20. For a comparison, characteristics of CB-1 and another LC blend CB-2, which contains neither non-mesomorphic nor chiral dopant and has a high phase-transition temperature ( $S_A - 54.2^{\circ}C - N - 59.8^{\circ}C - I$ ), are also shown in Table II. The LC blend CB-1 is not acceptable

because its heating margin parameter  $\Delta t_H$  is zero and its contrast ratio is too small. CB-2 has a larger contrast ratio than CB-1 but its writing time per line ( $t_{H1} + t_{S1}$ ) is too long. The LC blends CB-11 and CB-12 have practically favorable features, such as wide allowance of the driving condition, high contrast ratio and high writing speed.

## 6. SUMMARY

A non-mesomorphic dopant which has a large effect on the expansion of the temperature range of coexisting nematic-isotropic phases, improves the allowance of the driving condition as well as increases the contrast ratio. The expansion of the above-mentioned temperature range reduces the thermal stability of the liquid crystal. The parameter  $\Delta\beta$ , which quantifies the decrease in thermal stability of a liquid crystal, is shown to be useful to evaluate the effect to improve the allowance of the driving condition and the contrast ratio. Although chiral dopants improve the allowance of the driving condition and contrast ratio, the parameter  $\Delta\beta$  cannot be applied to them. In those cases, the twist force of chiral dopants has a large effect on the improvement.

The minimum signal voltage to make a transparent state is not changed by doping in the case of non-mesomorphic dopants. On the other hand, in the case of chiral dopants, the signal voltage increases with increasing the doping concentration. This also implies that there is a difference in the mechanism of the electro-thermo-optical effect between these two cases.

On the basis of the above-mentioned investigations, liquid crystal blends were developed. They have not only a wide allowance of the driving condition and high contrast ratio but also a high writing speed.

## Acknowledgment

The author would like to thank Dr. S. Matsumoto and Mr. Y. Kato for valuable discussion and his colleagues for their support in experimental assistance during this research.

## References

1. M. Hareng, S. LeBerre, R. Hehien and J. N. Perbet, SID International Symposium Digest of Technical Papers, p. 106 (1982).
2. G. N. Taylor and F. J. Kahn, *J. Appl. Phys.*, **45**, 4330 (1974).
3. A. Sasaki, N. Hayashi and T. Ishibashi, Proceedings of The 3rd International Display Research Conference (Japan Display '83) p. 494 (1983).
4. S. Matsumoto, M. Kawamoto and N. Kaneko, *Appl. Phys. Lett.*, **27**, 268 (1975).
5. H. Hatoh, Y. Kato and S. Matsumoto, Technical Report of The ITE of Japan, ED 838, IPD91-15, p. 37 (1984).